

PROPERTIES OF IN-100 PROCESSED  
BY POWDER METALLURGY

L.N. Moskowitz, R.M. Pelloux and N.J. Grant  
Department of Metallurgy and Materials Science  
Massachusetts Institute of Technology  
Cambridge, Massachusetts

Abstract

A powder metallurgy approach to the production of IN-100 has been shown to result in a fully dense, homogeneous alloy with excellent hot-workability. Small billets were prepared by compacting metal powders processed by inert-gas atomization, by vacuum-atomization, and by the rotating electrode process. The different powders are characterized by scanning electron microscopy, and size distributions as well as dendrite arm spacings are presented. Compaction of the powders was done by hot isostatic pressing and by hot extrusion. The mechanical properties of different billets are compared to the cast IN-100 as a function of the processing variables. Characterization of the hot workability of the powder processed IN-100 is first done by high strain rate testing, and finally by an investigation of the superplastic behavior at low strain rates in the temperature range from 1800°F to 2100°F. The rate of grain coarsening at 2270°F is shown to depend upon the size and amount of titanium carbide phase at the prior particle boundaries.

The excellent low temperature properties of IN-100 processed by powder metallurgy are related to the refinement of the grain size and microstructure and break-down of powder particle films obtained during atomization and hot extrusion. The stress-rupture properties at 1800°F, which are strongly dependent upon the grain size obtained during the 2270°F coarsening heat treatment, are slightly inferior to the properties of the cast alloy.

Introduction

The main goal of this work was to investigate the properties of a nickel-base superalloy processed by powder metallurgy. This material will be referred to as a P/M alloy as opposed to a cast alloy. Nickel base superalloys, widely used as components of modern gas turbines, consist of a solid-solution-hardened nickel-chromium matrix strengthened by an ordered gamma-prime ( $\text{Ni}_3(\text{Al}, \text{Ti})$ ) dispersed precipitate, and by some complex metal carbides. The metallurgy of these alloys has been reviewed by Decker (1) and Sims (2). The complexity of the alloy chemistry is such that severe segregation is always present in small as well as in large castings. Although the precipitated gamma prime phase goes into solution above about 2000°F, the carbide phases and the primary gamma prime do not re-solution until incipient melting has taken place at about 2300°F. Therefore, the hot plasticity of the cast alloys is severely limited even above 2100°F.

Since a prealloyed powder particle is an extremely small casting, segregation is restricted to each particle of powder. Cooling from the molten state is much faster for a powder particle ( $10^3$  °C/sec) than for a sand casting ( $10^0-10^{-2}$  °C/sec). As a consequence, the dendrite arm spacing and the volume fraction of large second phase particles are quite small, which will facilitate homogenization of the alloy. The mode of compaction of the powders can be selected from a wide variety of processes, such as sintering, hot isostatic compression, hot extrusion, etc., which can be tailored to

optimize the size and shape of the finished part. The fine-grained structure, achieved by the powder process, insures good ductility even for the brittle and hard-to-work alloy compositions.

Allen et.al. (3) made one of the first attempts to produce P/M ingots of Astroloy. To eliminate oxidation of individual powder particles, an "all-inert" method of powder production, collection and densification in an argon atmosphere was developed. Densification was performed by hydraulic pressing in a heated die, under a range of temperatures and pressures. Subsequent forgings of full scale discs yielded a structurally uniform product; however, the mechanical properties were inferior to those of conventional Astroloy forgings. The microstructure of the P/M alloy showed recrystallized grains and a network of small, discrete precipitates, identified as titanium carbide (TiC), along the prior particle boundaries.

Reichman et.al. (4) conducted a program to process superalloys from argon atomized powders with a low interstitial content. The two alloys studied were IN-100 and U-700, used respectively for cast turbine blades and wrought turbine discs. The consolidation techniques evaluated were vacuum hot pressing, forging, extrusion, hot isostatic pressing and spark sintering. Direct hot extrusion was found to be the best compaction process due to the rapidity of densification and the reproducibility of the processing variables. Hot isostatic pressing, while producing limited amounts of plastic deformation, was considered important for the fabrication of large forging or extrusion preforms. These processes will be discussed in more detail later. An evaluation of the final extruded product showed an ultrafine grain structure exhibiting superplastic behavior at high temperatures and low strain rates. An extremely large grain size structure was also achieved following some undisclosed thermomechanical treatment. This material exhibited stress-rupture properties superior to those of the cast and wrought alloys. The grain growth behavior leading to grain sizes larger than the original powder particles was attributed to the low contamination of the powder surface and low oxygen content of the densified product.

In a further investigation into the superplasticity of the extruded IN-100 powder, Reichman et.al. (5) showed that grain growth can also be achieved subsequent to superplastic deformation without an intermediate thermomechanical treatment. In order to obtain a very fine grain size (on the order of a few microns) which will lead to superplastic deformation, the powder compacts were extruded below the recrystallization temperature of the alloy. Adiabatic heating during extrusion leads to recrystallization and a fine-grained structure.

A practical method for fabricating high temperature alloys to close tolerances, utilizing the low strength and high ductility offered by the superplastic behavior of the alloys, was patented in 1970 under the name of "gatorizing" (6). It is claimed to apply to alloys in the cast condition, as well as to powder products. The process consists of working the alloy initially in compression at a temperature below, but approaching the recrystallization temperature and producing a very fine recrystallized grain size. Forging is done in hot dies, in an inert atmosphere, at an appropriately slow deformation rate. The part is then recrystallized and grain coarsening restores the high temperature strength. Production of full-scale compressor and turbine discs by the gatorizing process from IN-100 powder billets is described by Athey et.al. (7).

The mechanism of grain coarsening in the P/M alloy to the grain sizes of the cast alloy was studied more recently by Reichman et.al (8). A series of alloys were designed and tested with very low carbon contents, thereby eliminating the presence of carbides at grain boundaries and allowing easy grain growth. It was suggested that a final carburizing treatment can be easily accomplished to precipitate some carbides for grain boundary stability.

IN-100 was selected for our work since it is one of the highest strength cast nickel-base superalloys, very difficult to fabricate, with a high volume percent of gamma prime. Powders obtained by three different atomizing techniques were investigated: inert-gas atomization, vacuum atomization, and the rotating electrode process. The microstructure, grain growth, hot plasticity, and mechanical properties of billets compacted by hot isostatic pressing and hot extrusion were investigated and compared

to the cast alloy.

### Characterization of Metal Powders

Three types of prealloyed IN-100 powders were evaluated. They will be referred to as FM powder (inert-gas atomization), HM powder (vacuum atomization), and NM powder (rotating electrode process). In inert-gas atomization, a pre-alloyed vacuum cast ingot is vacuum remelted, and atomized by a stream of high purity argon gas. The size of the spherically solidifying particles is controlled by the atomizing parameters. In vacuum atomization, a vacuum remelted alloy is pressurized and saturated with a soluble gas such as hydrogen. Atomization is obtained by dissociation of the liquid metal-gas mixture in a vacuum chamber. As the metal rises, the stream is exploded by the gas escaping the liquid metal, and a coarse powder is produced. The rotating electrode process (9) uses a consumable rotating electrode of the alloy which is continually melted by an arc from a stationary tungsten electrode. Powder production takes place in a chamber filled with high purity helium, in which fine spherical droplets are flung off by centrifugal force. The powder particle size is controlled by varying the electrode diameter and the electrode rotating speed. The principles behind the production and control of powder particles have been reviewed by Orr (10).

Coarse, spherical IN-100 powders could not be produced by steam atomization due to the high titanium and aluminum contents of the alloy. The coarse powder obtained was sharp and flaky with a thin, adherent oxide film. The shapes of these powders are unfavorable for processing since they present many reentrant cavities and folds in cleaning, and have a very low packing density in hot isostatic pressing or extrusion cans.

Chemistries, size ranges and screen analyses of the three powders used are presented in Tables I and II. With the exception of FM powder, all contain less than 100 ppm of oxygen and show little oxygen pick-up during powder production. Typical powder particles viewed by scanning electron microscopy are shown in Figures 1, 2 and 3. FM powders are predominantly spherical in shape with many fine particles attached to coarser particles. The dendritic structure can be seen in relief only on the surface of the larger particles. HM powders are much more irregular in shape, and consist of flakes as well as droplets. Some surfaces contain protrusions, and the dendritic structure can be identified. NM powders are much smoother and well-rounded, and more uniform in size. The surface appearance indicates a much cleaner powder. Polished and etched cross-sections of powder particles of each type are presented in Figures 4, 5 and 6. The average secondary dendrite arm spacing in FM powder is 2 microns, in HM is 6 microns, and in NM is 3 microns, and varies little in each heat. For a discussion of the variation in dendrite arm spacing with cooling rate, see Ref. 13. A semi-qualitative analysis of the surface and interior of the particles was done with a non-dispersive X-ray attachment to the SEM. There was no marked difference in chemistry between the core and the outside surface of the powders.

Table 1 - IN-100 Chemistries (w/o)

	Ni	Cr	Co	Mo	Al	Ti	C	B	Zr	V	Fe	Mn	Si	S	
As-Cast	Bal.	10.5	15.4	3.02	5.55	4.72	.16	.015	.06	1.05	.94	<.10	.05	.007	Oxygen
FM Powder	Bal.	9.54	13.97	3.70	5.65	4.82	.17	.014	--	--	--	--	--	--	Ingot 108
HM Powder	Bal.	10.5	15.4	3.02	5.55	4.72	.16	.015	.06	1.05	.94	<.10	.05	.007	50
NM Powder	Bal.	9.40	15.18	3.08	5.81	4.82	.178	.016	.06	.99	<.01	<.10	<.10	.001	74

Table 2 - Size Range and Screen Analysis (% retained)  
of the Powders as Received from the Manufacturers

	FM Powder	HM Powder	NM Powder
Size Range (microns):	-250 + 44	-707 + 74	-500 + 44
Mesh:			
-25 + 35	0.0	4.6	0.0
-35 + 60	0.5	43.0	4.3
-60 + 100	1.3	24.0	58.0
-100 + 200	43.3	28.4	29.5
-200 + 325	23.3	0.0	6.6
-325	31.6	0.0	1.6

#### Powder Consolidation

Hot isostatic pressing (HIP) is a consolidation process involving the application of a hydrostatic pressure by a gas (usually argon or helium) at elevated temperatures to evacuated, canned powders. With the advent of modern high-pressure equipment, large diameter parts with complex geometries can be fabricated (11). It has been shown that full density can be achieved by HIP processing, (12, 13, 14) with good control over microstructure and chemistry. While the final structure is isotropic, only limited amounts of plastic deformation can be achieved during pressing. The basic requirement of the canning material is high plasticity at the forming temperature. Thin gauge low alloy carbon steel is often used and contamination of the core is negligible (14).

Direct powder extrusion, in evacuated cans, offers both hot consolidation and hot mechanical working to yield a fully dense wrought material. Interparticle shearing promotes a break-up of prior particle boundaries as well as enhancing bonding. Hot extrusion of superalloy powders has been carried out over a wide range of temperatures and extrusion ratios (4,15). The parameters involved in the selection of the correct temperatures, reduction ratios, canning material and heat treatment are discussed by Bufferd (15). In general, the canning material must be as strong as the powder at the extrusion temperature, and it should be easy to remove after processing.

In this study, small billets of IN-100 were prepared by the above consolidation techniques, as listed below:

- 1) Hot isostatically pressed FM powders, 1" x 1-1/2" x 20". Pressed at 2320°F and 25,000 psi for one hour.
- 2) Hot isostatically pressed HM powders, extruded to 3/4" diameter rod. Pressed at 2300°F and 15,000 psi for one hour; extruded at 2000°F with a 12:1 reduction.
- 3) Direct extruded FM and NM powders (2 bars), 1/2" diameter x 7' in length. Extruded at 2150°F with a 20:1 reduction.

#### Results and Discussion

##### Microstructure

All metallographic samples were polished to 0.05 micron alumina in distilled water. The different etching solutions given in Table 3 attack gamma prime, leaving the carbides in relief and gamma prime depressed relative to the gamma matrix. Etchant no. 1 gave

the best overall structural definition, while etchant no. 4 was used to delineate the dendritic structure. All were applied by immersion and the etching times are indicated.

Table 3 - Etchants

1. 92 HCl  
5 HNO<sub>3</sub>  
3 H<sub>2</sub>SO<sub>4</sub> - add last  
immersion (~30 sec)  
good for IN-100 microstructure and Ni<sub>3</sub>(Al,Ti)
2. 60 glycerine  
30 HCl  
15 HNO<sub>3</sub>  
immersion (~120 sec)  
good for IN-100 microstructure and Ni<sub>3</sub>(Al,Ti)
3. Kalling's etch  
5g CuCl<sub>2</sub> · 2H<sub>2</sub>O  
100 ml C<sub>2</sub>H<sub>5</sub>OH  
100 ml HCl  
immersion (~200 sec)  
good for IN-100 microstructure and grain structure
4. 70 HCl  
10 H<sub>2</sub>O<sub>2</sub> (30%)  
HF (activator)  
immersion (~20 sec)  
good for IN-100 dendrite structure

Two-stage carbon-chromium replicas were prepared from cellulose acetate first stage replicas. The shadowing angle was approximately 30°.

In order to compare the structures and properties of the powder product to the cast alloy, an investment casting of IN-100 was made into 24 3/8" diameter thread tensile bars. The casting was made from a vacuum cast ingot of IN-100 (see Table 1 for the chemical analysis). The bar was remelted under an argon atmosphere, and cast at 2730°F into a mold at 1500°F. The average grain size in the cast bars is 1500 microns, with about five grains per diameter.

The average secondary dendrite arm spacing in the cast IN-100 tensile bars is 28 microns, as seen in Figure 7, and the typical cast nickel-base superalloy structure is evident in Figure 8. The average size of the matrix gamma prime particles is about 1.5 microns.

Figure 9 shows the structure of the hot isostatically pressed bar of FM powder. Recrystallization has taken place within the particle boundaries, but there is no sign of plastic deformation in individual powder particles. An almost continuous film of second phase precipitates surrounds each particle. This, as well as the gamma prime morphology and size (about 0.7 microns), can be seen more readily in the replica electron micrographs of Figure 10. Nondispersive X-ray analysis showed the surrounding phase to be rich in titanium, a strong carbide forming element, and to contain a much smaller concentration of aluminum. In order to make a positive identification, carbon

extraction replicas were prepared. A 10% bromine in alcohol solution was used to dissolve the matrix after direct evaporation of a carbon film on the polished and well-etched sample. Electron diffraction of the extracted replicas, using a 200 kv electron beam, showed the phase to be titanium carbide. The presence of aluminum in the carbides is most likely related to an oxide phase identified by Moyer in similar work on U-700 (16).

Upon examination of the bar of HM powder which had been hot isostatically pressed and then extruded, the entire length was found to contain numerous holes and cavities. This porosity is attributed to the presence of some residual hydrogen, remaining in the powders after vacuum atomizing, and vacuum degassing prior to hot pressing.

The microstructure of the as-extruded bars is shown in Figures 11 (FM powder) and 12 (NM powder). The particles have been well deformed, and a recrystallized grain size of about 8 microns is evident in both bars. Large carbides within the particle boundaries can be seen in the bar extruded from NM powders. These carbides were present in the original powders. The prior particle boundaries of the FM powder extrusion are still delineated by a second phase, although not to the extent that it was in the HIP material. In the NM powder bar, this effect is even smaller. The average gamma prime particle size after extrusion is about 0.2 microns in each alloy.

#### Grain Coarsening

In order to see if significant grain growth could easily occur past the prior particle boundaries, a series of grain coarsening experiments were run. Tests initially performed at 2300°F showed evidence of incipient melting, and 2270°F was selected as an optimum coarsening temperature. The samples from the FM powder extrusion showed substantially less grain growth than those from the NM powder, indicating that the surrounding carbide phase can slow down grain growth markedly. In both alloys, however, grain boundaries were able to grow past the prior particle boundaries. For the FM powder extrusion, the average grain size was about 50 microns after 24 hours at 2270°F, with grains as large as 100 microns. For the NM extrusion, after the same treatment, an average grain size of about 100 microns was measured, with grains as large as 200 microns (Figure 13).

#### Mechanical Properties

Room Temperature Properties: The room temperature tensile properties and Rockwell C hardness values for the different materials are presented in Table 4. The excellent room temperature tensile properties of the as-extruded material are attributed to the refinement of the microstructure during atomization and the break-down of powder particle films during hot extrusion. There is no difference between transverse and longitudinal hardness, but the high hardness values correlate well with the high tensile properties. The tensile ductilities of all the P/M alloys are excellent considering the strength levels and compared to the ductility of the cast alloy.

Table 4 - IN-100 Room Temperature Properties

Material	Hardness ( $R_c$ )	.2% YS (ksi)	UTS (ksi)	% elong.	% RA
As-Cast	32	136	143	4	8
As-HIP +EXTR (HM)	41	-	-	-	-
As-HIP (FM)	49	137	163	8	10
As-EXTR (FM)	43	175	244	20	16
As-EXTR (NM)	43	171	238	21	17
As-Grain Coarsened(NM)	33	137	188	14	7

Hot Plasticity Tests: Characterization of the hot workability of the powder processed IN-100 was first done by high strain rate testing and finally by an investigation of the superplastic behavior at low strain rates. The high speed tensile testing was performed in a Nemlab high strain rate machine which has a stroke of 2-1/2", and is capable of reaching a maximum load of 5000 pounds within 20 milliseconds, with maximum deformation rates on the order of  $20 \text{ sec}^{-1}$ . It has been used successfully as a means of simulating hot working operations, to find the optimum conditions of strain rate and temperature to forge high strength materials (17,18,19). A complete discussion of the operation and calibration of the machine can be found in the work of Cederblad (17). An 11 inch radiant split furnace was used to reach a maximum temperature of 2200°F in five minutes. Thermocouples were spot welded directly on the specimens. Tests were conducted on the as-cast, as-HIP, and as-extruded materials at 1900°F, 2000°F, 2100°F and 2200°F, the temperature range of conventional superalloy forging. The holding time at temperature was less than five minutes in all cases so as to limit structural changes and make the tests more reproducible.

The stress versus rupture time and stress versus average deformation rate showed suitable linear relationships on log-log plots. Typical curves for the as-extruded powders are shown in Figures 14 and 15. The ductility, measured as elongation after fracture, is presented for each test. The most noticeable difference in the behavior of the three materials tested is the sharp change in slope exhibited by the extruded product at rates below about  $10^{-1} \text{ sec}^{-1}$ . This break in the slope, indicating a change in structure, deformation or fracture mode, was not exhibited by either the cast or HIP alloy.

Poor ductility (<5% elongation) was exhibited at all temperatures by the cast and HIP bars. The ductility of the extruded material, however, is seen to increase markedly at slower deformation rates, especially at 2100°F. Total elongations as a function of deformation rate are plotted in Figure 16.

This behavior is identical to that shown by the work of Greene (20) and Cederblad (17) on cast Udimet 700 and Nimonic 115, respectively. It was found that the ductility of these nickel-base superalloys increases as the strain rate decreases at all test temperatures, but ductility is maximized at 2100°F at all strain rates. The increase in ductility as the temperature is raised to 2100°F is due to the increased amounts of gamma prime going into the gamma solid solution. The decrease in ductility at temperatures greater than 2100°F is due to a structural change brought about by recrystallization.

A typical fracture cross-section of the hot isostatically pressed FM powder is shown in Figure 17. The bar failed by interparticle separation, explaining the low ductility of this material. The influence of the surrounding titanium carbide and oxide phases in initiating fracture at the powder particle boundaries was obviously great. A cross-section of an extruded FM powder test bar is shown in Figure 18. The material exhibits extensive intergranular cracking, accounting for part of its higher ductility.

A comparison of the high strain rate stress levels showed the extruded material to be stronger or as strong as the cast material, with the hot pressed material the weakest of the three. At deformation rates below about  $10^{-1} \text{ sec}^{-1}$ , however, the stress levels in the extruded product fall rapidly below both of the other materials, an effect most pronounced at 2100°F.

Superplastic Deformation of As-Extruded Alloys: This extreme sensitivity of the deformation stress and ductility on temperature, strain rate and structure led to a series of low strain rate tensile tests, to investigate the superplastic behavior of the extruded material which had been reported by Reichman et.al. (5). High temperature tensile tests were performed on the as-extruded alloys over a range of strain rates from .005 to .5  $\text{min}^{-1}$  at 1800°F, 1900°F, 2000°F and 2100°F.

Figure 19 shows the total elongation that can be obtained at different strain rates at 1900°F, as compared to an undeformed tensile bar of one inch gauge length.



The results are plotted on log-log coordinates as true flow stress vs. strain rate in Figure 20. It was found that the initial holding time at temperature had a marked effect on the tensile behavior, especially at the lower temperatures. For this reason, soaking times of 30 minutes at temperature were used before beginning each test. The slopes of the curves in Figure 20 are approximately the same and equal to 0.5 below about  $10^{-1} \text{ min.}^{-1}$ . This value of the slope was taken as the strain rate sensitivity exponent,  $m$ , in  $\sigma = K\dot{\epsilon}^m$ , where  $\sigma$  = flow stress,  $K$  = constant, and  $\dot{\epsilon}$  = strain rate. The activation energy for the deformation process was determined from an Arrhenius plot at two stress levels. A constant activation energy of approximately 98 kcal/mole was found. These results are in agreement with the work of Reichman et.al. (5).

The microstructure of a superplastically deformed tensile bar is shown in Figure 21. The most noticeable change exhibited is the extreme growth of the gamma prime particles, from about 0.2 micron to an average size of one micron.

Creep Testing: 1800°F stress-rupture tests were conducted on the extruded material from FM and NM powders, and the grain coarsened (24 hours at 2270°F - air cooled) NM powder material. To optimize the creep strength, the as-extruded material was overaged at 1800°F for 24 hours, and the grain-coarsened material at 1825°F for 20 hours. The stress-rupture results are compared to stress-rupture properties of fine and coarse-grained cast IN-100 (21) in Figure 22. The total elongations are presented for each test. The extruded material (average grain size of 8 microns) exhibits stress-rupture properties far inferior to that of the cast material, as a result of the fine grain size. The 100 micron grain-coarsened material shows stress-rupture properties beginning to approach those of the cast material. The total elongations observed in the material, however, are below those of the cast alloy. The difference in stress-rupture strength should be compensated for by improved fatigue properties due to the finer grain size and size of the second phase particles in the P/M alloy.

Some current work with low-carbon (.02%) P/M IN-100 alloys has shown that easy grain growth to cast grain sizes is possible. A hot isostatic pressing of these powders at 2300°F and 27,700 psi for one hour yielded a recrystallized grain size of about 500 microns with good 1800°F stress-rupture properties in the as-HIP condition. It is hoped that through proper processing of these low carbon P/M alloys, the creep and fatigue properties will prove to be superior to those of the cast alloy.

### Conclusions

1) A powder metallurgy approach to the production of a highly alloyed, cast nickel-base superalloy results in a fully dense, homogeneous alloy with excellent hot-workability. The control over dendrite arm spacing, phase distribution and grain size is made possible by proper choice of prealloyed powder particles, consolidation methods and parameters.

2) The extruded P/M alloys show much better mechanical properties than do the hot isostatically pressed alloys. This is a result of the extensive interparticle shearing during hot extrusion, which promotes the break-up of prior particle boundaries and enhances bonding. The prior particle boundaries in the HIP product are delineated by an almost continuous film of titanium carbide and oxides, which retards grain growth and results in poor high temperature properties.

3) Inert-gas atomized powders and rotating electrode process powders show roughly equal properties after extrusion. Grain growth at 2270°F occurs more easily in the R.E.P. powder extrusion, which contains less surrounding carbide phase, than in the inert-gas atomized powder extrusion. In both materials, however, grain boundaries were able to grow past the prior particle boundaries.

4) The excellent room-temperature tensile properties of the as-extruded material are attributed to the refinement of the grain size and microstructure and break-down of the powder particle films during atomization and hot extrusion.

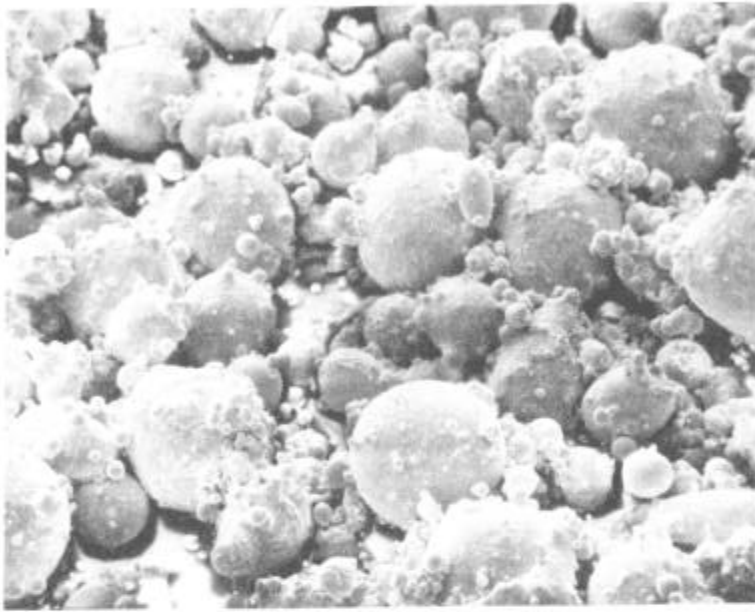
5) The ultra-fine grain structure resulting after extrusion and recrystallization, enables low strain rate, superplastic deformation of the P/M alloy to be employed as a close-tolerance fabrication procedure.

6) The stress-rupture properties at 1800°F are strongly dependent upon the grain size. Through use of a low-carbon P/M alloy of IN-100, easy grain growth is possible to typical cast grain sizes, and high-temperature stress-rupture properties should greatly improve.

## References

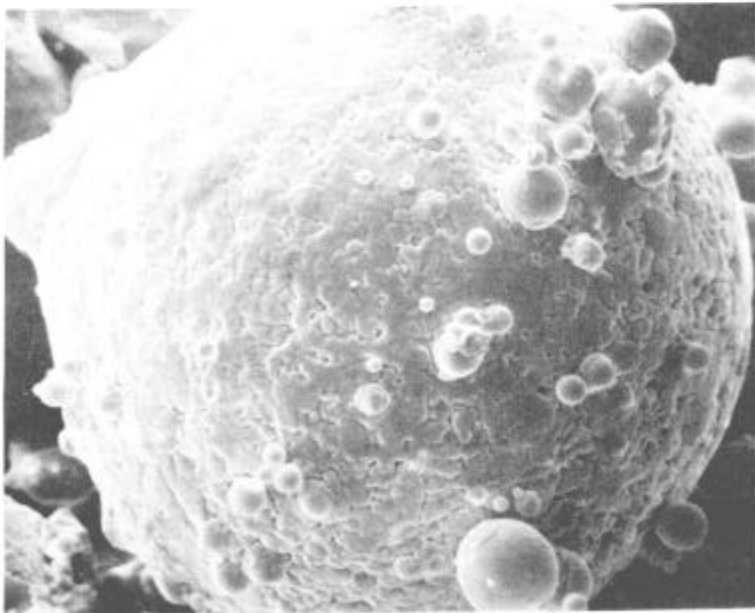
1. R.F. Decker: "Strengthening Mechanisms in Nickel-Base Superalloys", Market Development Department, International Nickel Company.
2. C.T. Sims: "A Contemporary View of Nickel-Base Superalloys", J. of Metals, Oct., 1966.
3. M.M. Allen, R.L. Athey, J.B. Moore: "Application of Powder Metallurgy to Superalloy Forgings", Metals Engineering Quarterly, Feb., 1969, p. 20.
4. S.H. Reichman, B.W. Castledine, J.W. Smythe: "Superalloy P/M Components for Elevated Temperature Applications", SAE Congress, Detroit, Michigan, Jan., 1970.
5. S.H. Reichman and J.W. Smythe: "Superplasticity in P/M IN-100 Alloy", Int. J. of Powder Met., 6, 1970, p. 65.
6. J.B. Moore, J. Tequesta, R.L. Athey: "Fabrication Method for the High Temperature Alloys", U.S. Patent 3,519,503, July 7, 1970.
7. R.L. Athey and J.B. Moore: "Development of IN-100 Powder Metallurgy Discs for Advanced Jet Engine Application", 18th Sagamore Army Materials Research Conference, August, 1971.
8. S.H. Reichman and J.W. Smythe: "New Developments in Superalloy Powders", Modern Developments in Powder Metallurgy, Hausner, ed., Vol. 5, Plenum Press, 1970, p. 73.
9. A.R. Kaufman: "Method and Apparatus for Making Powder", U.S. Patent 3,099,041, July 30, 1963.
10. C. Orr: Particulate Technology, Macmillan, New York, 1966.
11. H.D. Hanes: "Hot Isostatic Pressing of High Performance Materials", 18th Sagamore Army Materials Research Conference, August, 1971
12. Semi-Annual Technical Report No. 1, ARPA, Contract No.: DAHC15 70 C 0283, January, 1971.
13. Semi-Annual Technical Report No. 2, ARPA, Contract No.: DAHC15 70 C 0283, June, 1971.
14. Semi-Annual Technical Report No. 3, ARPA, Contract No.: DAHC15 70 C 0283, January, 1972.
15. A.S. Bufferd: "Complex Superalloy Shapes", 18th Sagamore Army Materials Research Conference, August, 1971.
16. K.H. Moyer: "A Correlation of Mechanical Properties of Sintered U-700 Powder with Particle Boundary Morphology", Modern Developments in Powder Metallurgy, Hausner, ed., Vol. 5, Plenum Press, 1970, p. 85.

17. N. Cederblad: "Hot Deformation of Nimonic 115 at High Strain Rates", S.M. Thesis, MIT, August, 1971.
18. J. Dhosi, L. Morsing, N.J. Grant: "The Effect of Bismuth on the Hot Plasticity of Two Stainless Steels at High Temperatures and High Strain Rates", Eighth Mechanical Working and Steel Processing Conference, AIME, N.Y., 1967.
19. R.H. Kane and N.J. Grant: "Recrystallization and Grain Refinement", Ultrafine-Grain Metals, J. Burke and V. Weiss, ed., Syracuse University Press, 1970, p. 163-179.
20. B.N. Greene: "High Strain Rate Deformation of Udimet 700", S.M. Thesis, MIT, January, 1966.
21. "Engineering Properties of IN-100", International Nickel Company.



138x

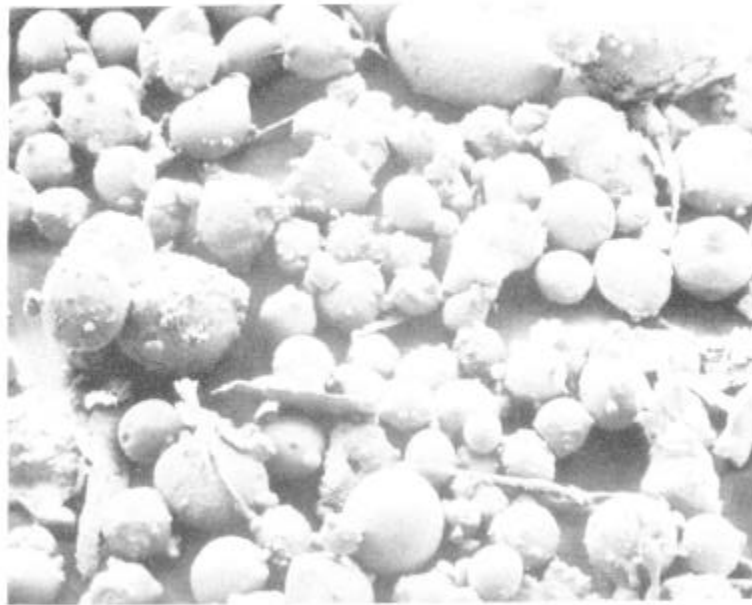
(a)



680x

(b)

Figure 1. As-Received FM Powders as Viewed in SEM



24x

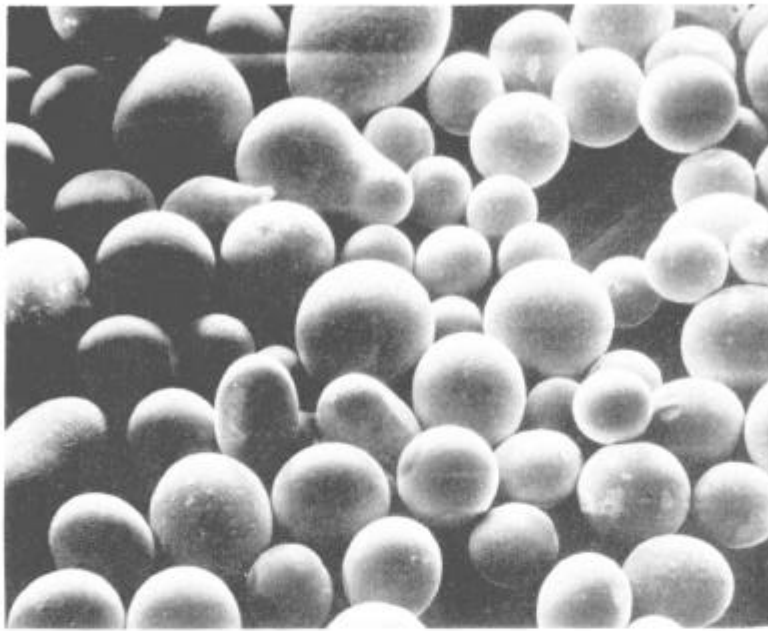
(a)



245x

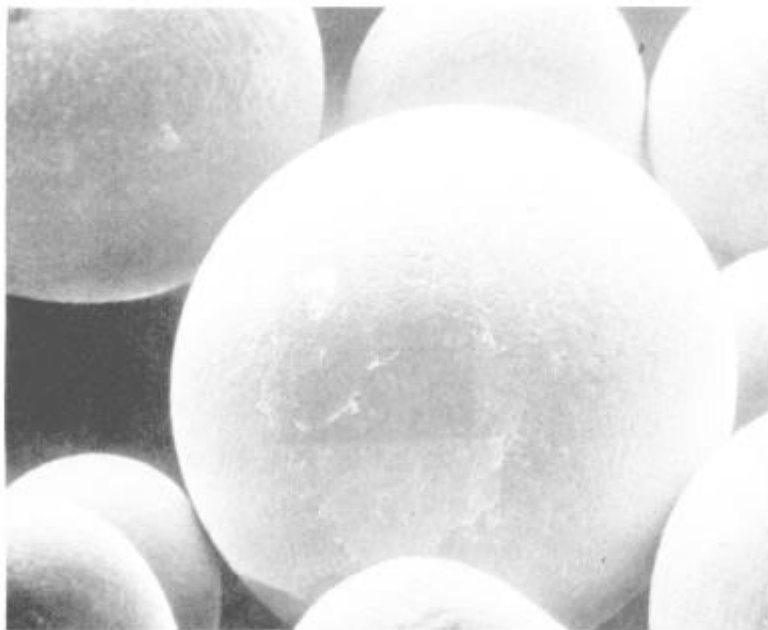
(b)

Figure 2. As-Received HM Powders as Viewed in SEM



63x

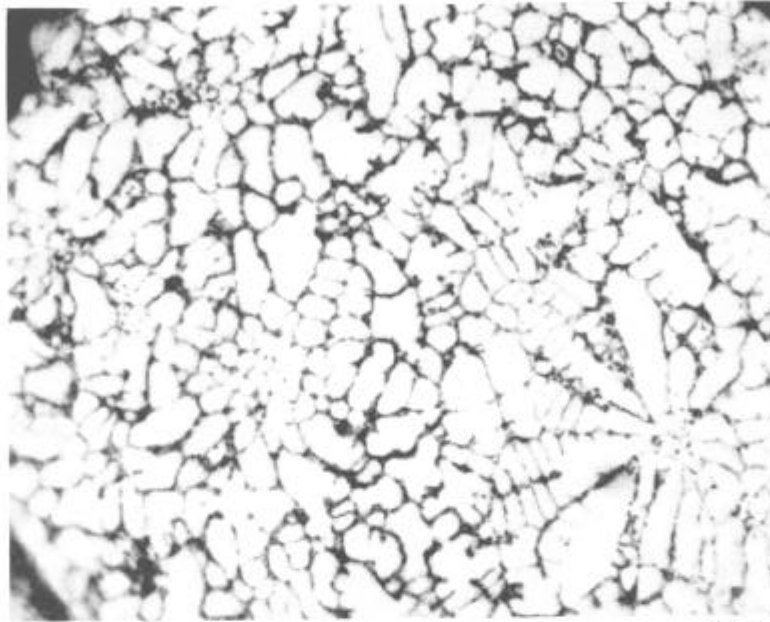
(a)



253x

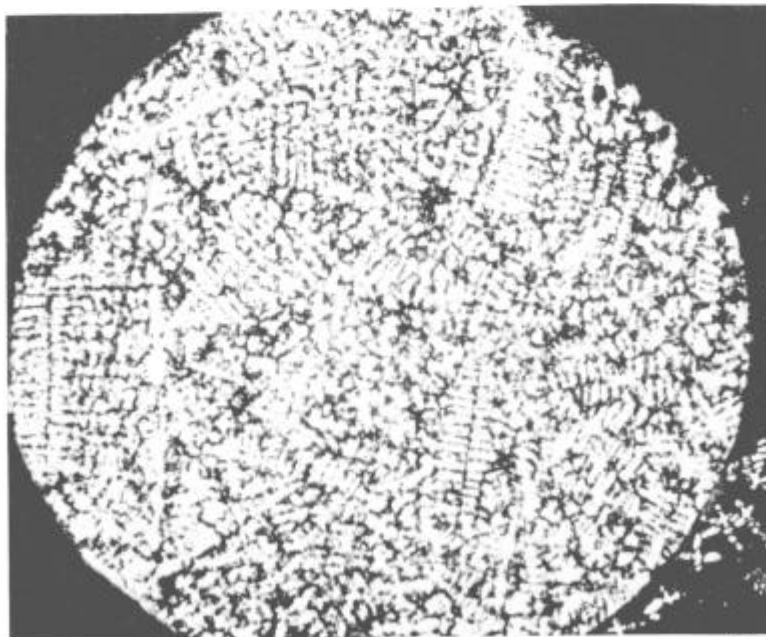
(b)

Figure 3. As-Received NM Powders as Viewed in SEM



500x

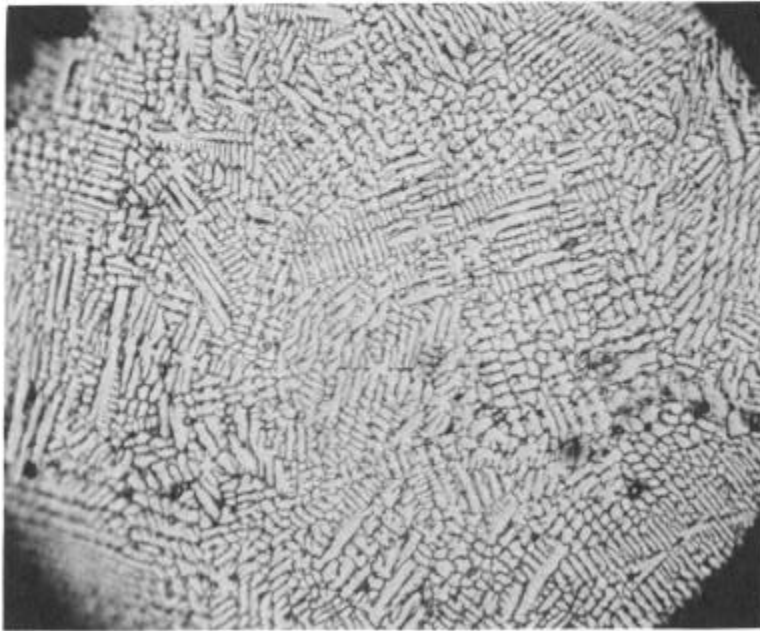
Figure 4. Polished and Etched Section of As-Received FM Powders Showing Dendritic Structure



50x

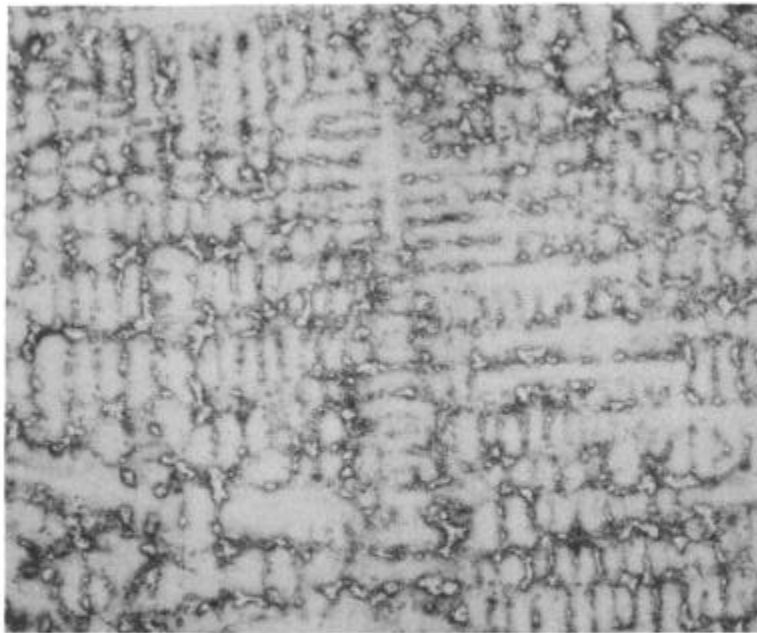
Figure 5. Polished and Etched Section of As-Received HM Powders Showing Dendritic Structure





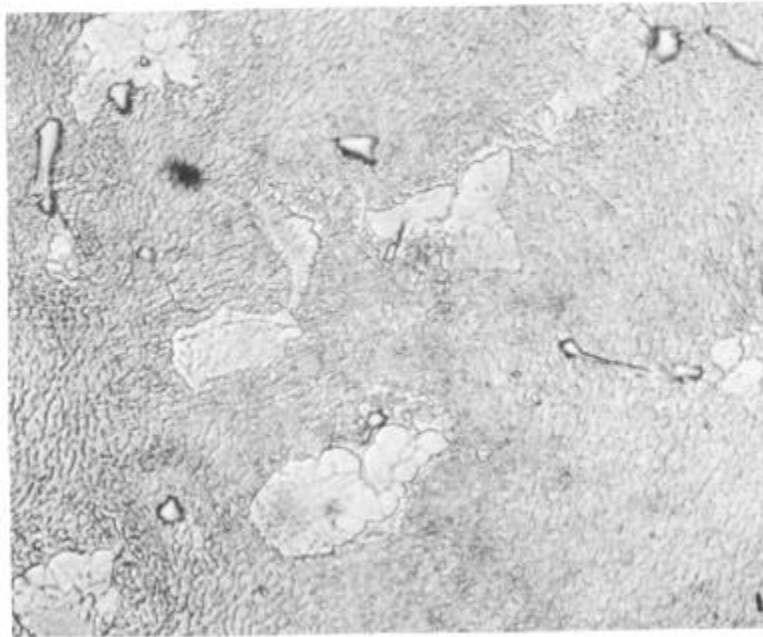
200x

Figure 6. Polished and Etched Section of As-Received NM Powders Showing Dendritic Structure



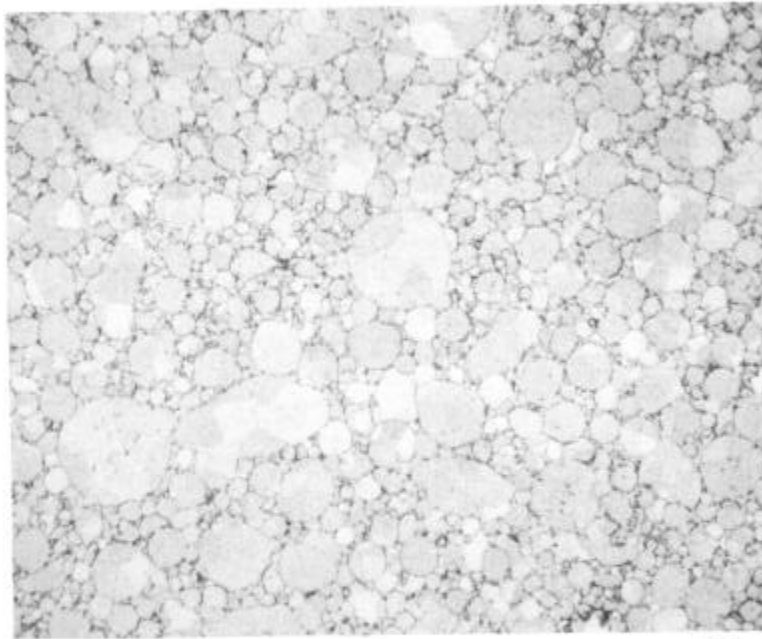
100x

Figure 7. Polished and Etched Cross-Section of As-Cast Tensile Bar Showing Dendritic Structure



1000x

Figure 8. As-Cast IN-100 Microstructure



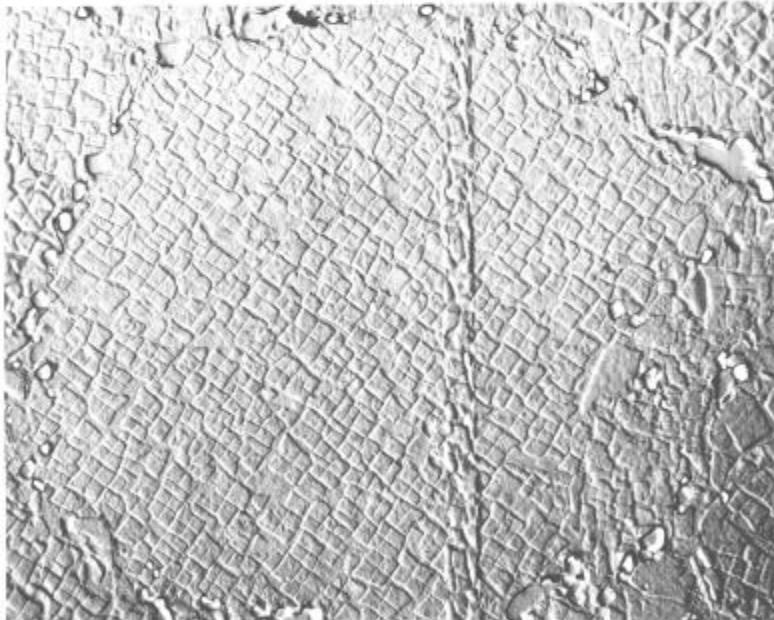
100x

Figure 9. As-HIP FM Powder



4000x

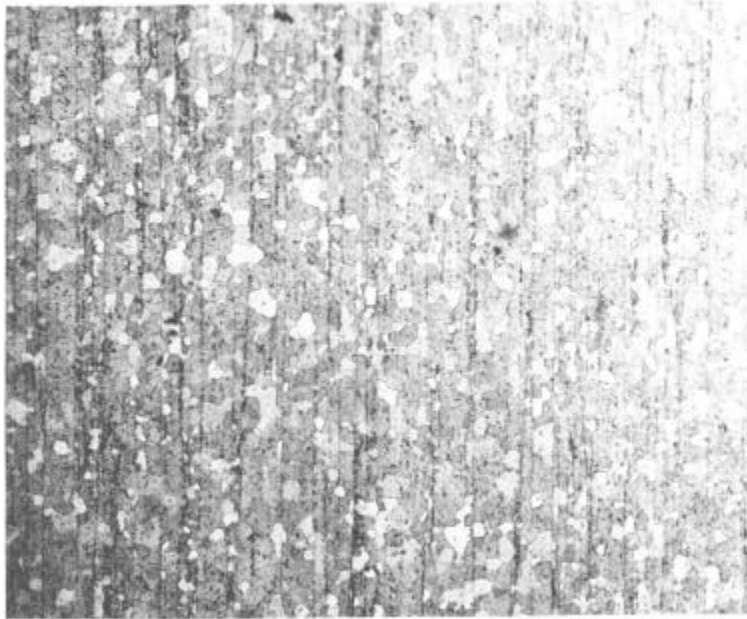
(a)



5000x

(b)

Figure 10. Replica Electron Micrographs of As-HIP FM Powder Showing Extensive Carbide Phase Surrounding Prior Particle Boundaries



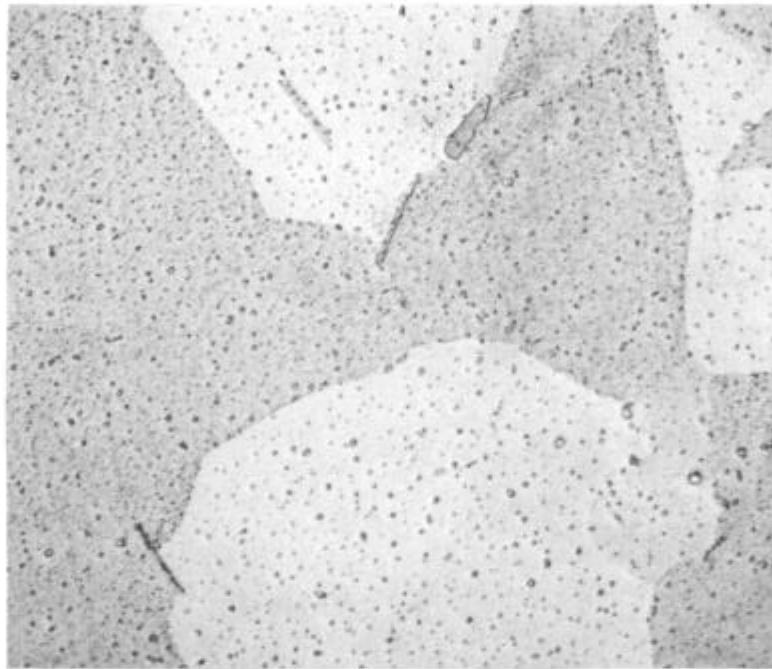
200x

Figure 11. Longitudinal Section of As-Extruded FM Powder



200x

Figure 12. Longitudinal Section of As-Extruded NM Powder



500x

Figure 13. Grain-Coarsened NM Powder Extrusion. 24 Hours at 2270°F

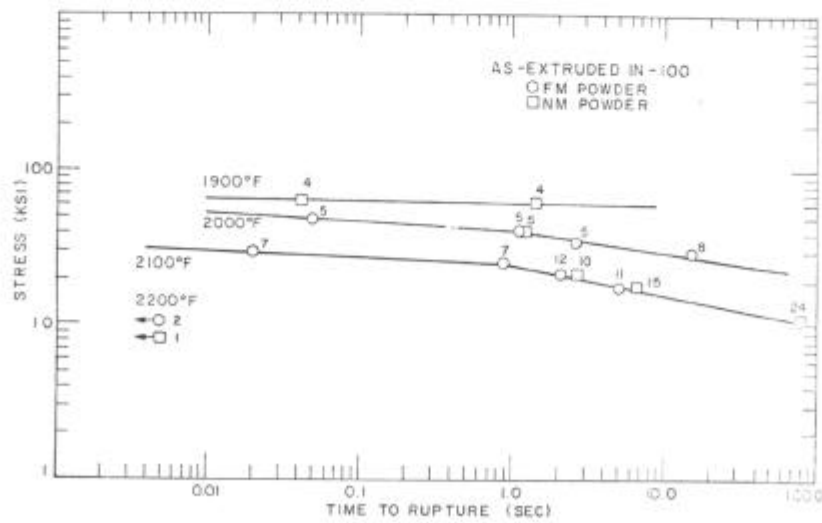


Figure 14. High Strain Rate Log Stress vs. Log Rupture Time at Various Temperatures for As-Extruded IN-100

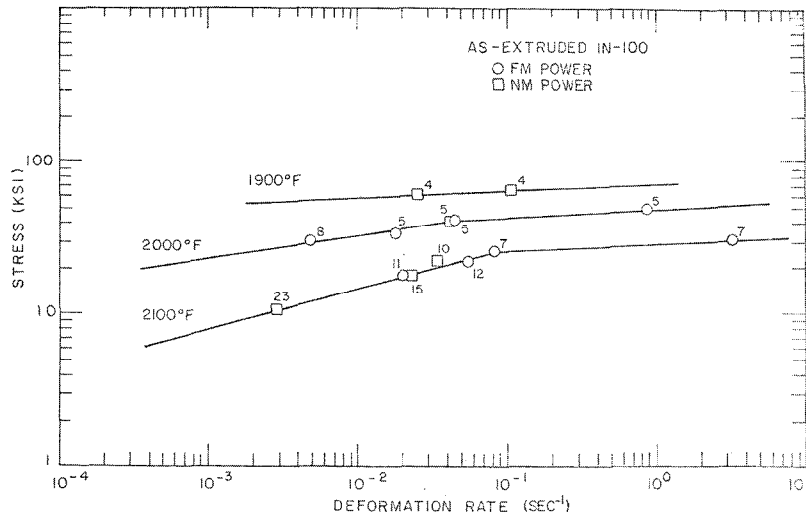


Figure 15. High Strain Rate Log Stress vs. Log Deformation Rate at Various Temperatures for As-Extruded IN-100

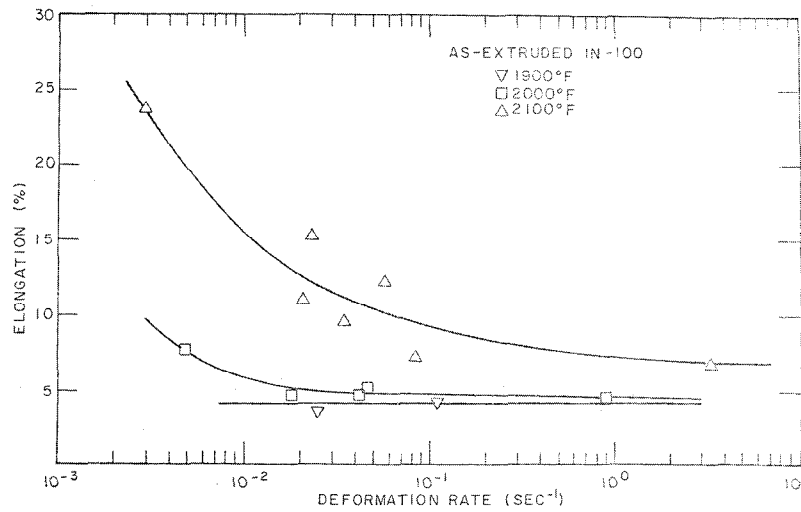


Figure 16. High Strain Rate Effect of Deformation Rate on Elongation at Various Temperatures for As-Extruded IN-100

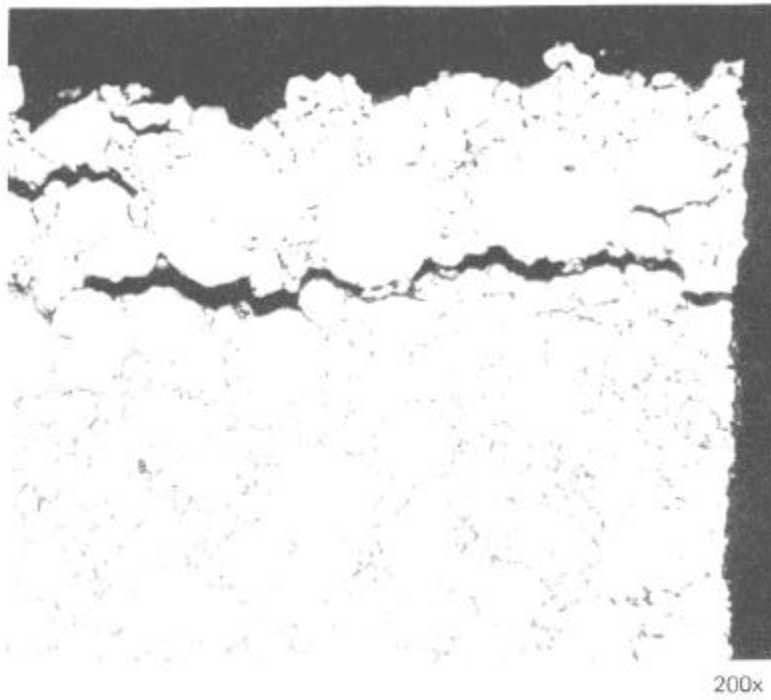


Figure 17. High Strain Rate Fracture Cross-Section of HIP FM Powder Test Bar Pulled at 2100°F. Polished.

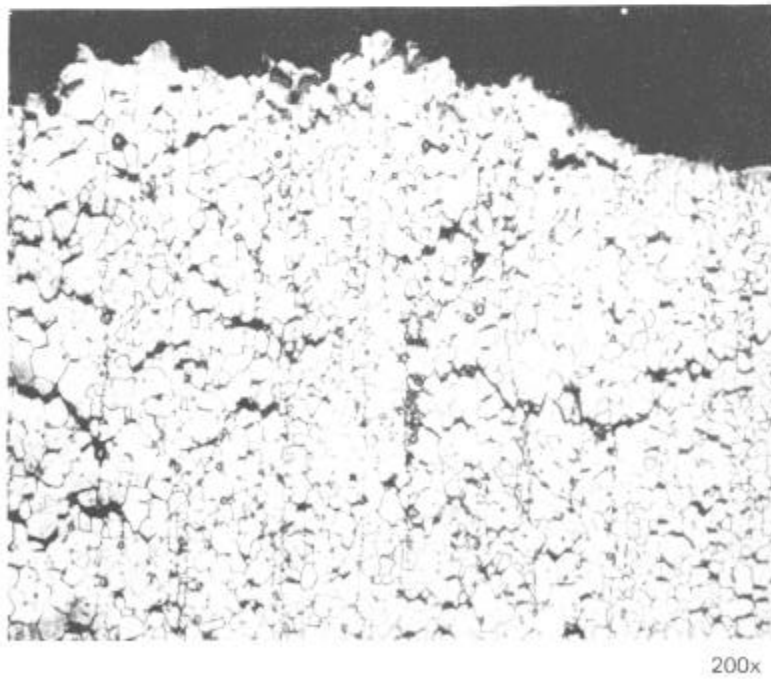


Figure 18. High Strain Rate Fracture Cross-Section of Extruded NM Powder Test Bar Pulled at 2100°F. Polished and Etched



Figure 19. As-Extruded Test Bars Superplastically Deformed at 1900°F at Strain Rates From 0.5 min<sup>-1</sup> to 0.01 min<sup>-1</sup>. Bar at top is Size of Undeformed Tensile Specimen

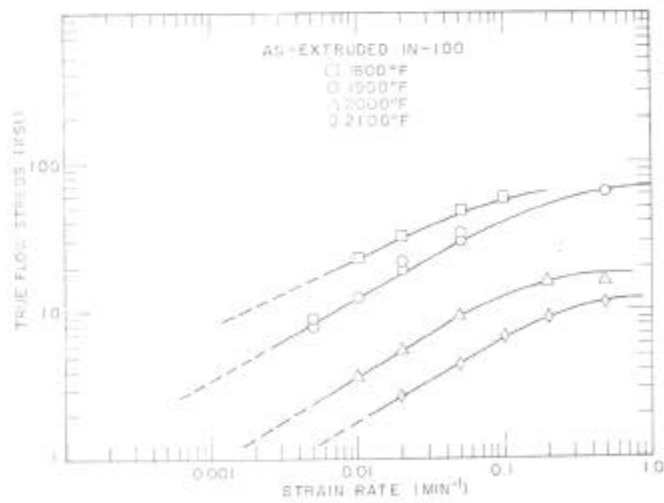
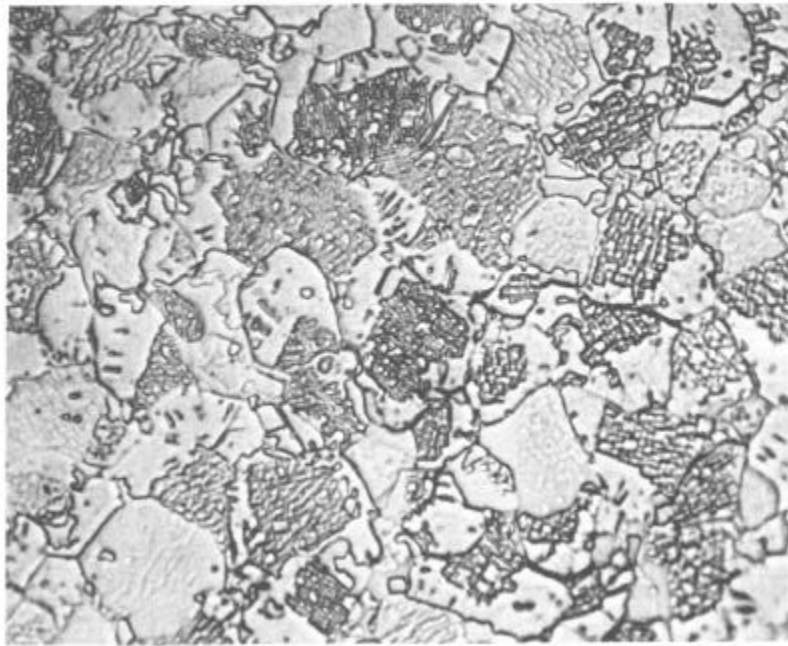


Figure 20. Superplastic Deformation of As-Extruded IN-100 at Various Temperatures Plotted as Log True Flow Stress vs. Log Strain Rate





1000x

Figure 21. Microstructure of Superplastically Deformed As-Extruded Material Pulled at 1900°F

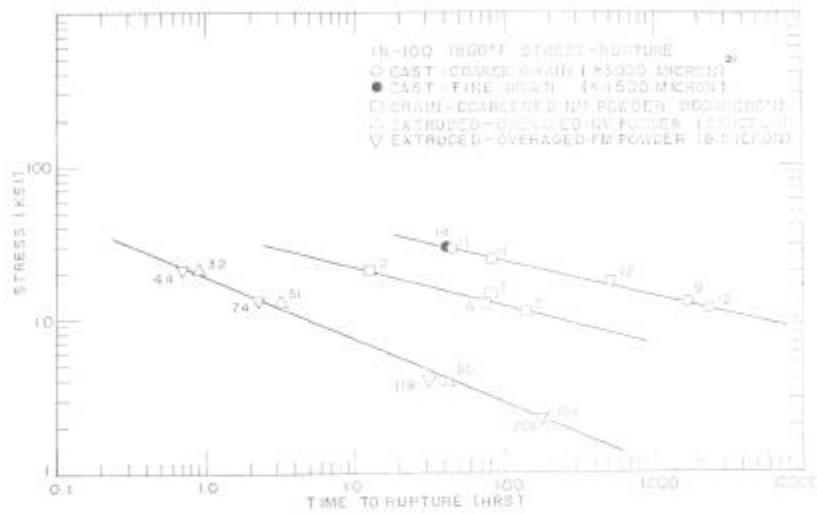


Figure 22. 1800°F Stress-Rupture Properties for Various Grain Sizes of Cast IN-100 and Extruded IN-100 Powders